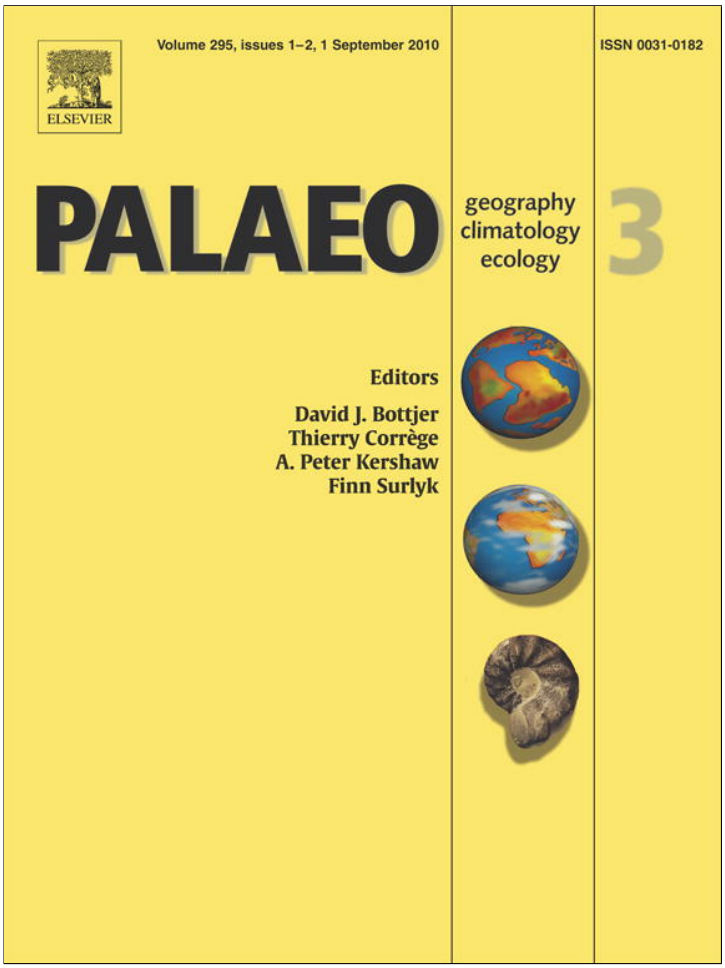

Palaeogeography, Palaeoclimatology, Palaeoecology 295 (2010) 76–88

Contents lists available at ScienceDirect

Palaeogeography, Palaeoclimatology, Palaeoecology

journal homepage: www.elsevier.com/locate/palaeo

Atmospheric susceptibility to wildfire occurrence during the Last Glacial Maximum and mid-Holocene

F. Justino [a,*], W.R. Peltier [b], H.A. Barbosa [c]

[a] Universidade Federal de Viçosa, Departamento de Engenharia Agrícola P.H.Rolfs S/N, +55 31 3899 1870 Viçosa, MG, Brazil, 36570 000
[b] University of Toronto, Dept. of Physics, 60, St. George Street, Toronto, Ont., Canada M5S 1A7
[c] Universidade Federal de Alagoas, Instituto de Ciências Atmosféricas ICAT, Campus A. C. Simões, BR 104 Norte km 97 Tabuleiro do Martins 57072-970 - Maceio, AL, Brazil

ARTICLE INFO

Article history:
Received 24 November 2009
Received in revised form 23 April 2010
Accepted 23 May 2010
Available online 16 June 2010

Keywords:
Paleofire
Climate changes
Last Glacial Maximum
Mid-Holocene

ABSTRACT

Based on coupled climate model simulations the impact of anomalous climate forcing on the environmental vulnerability to wildfire occurrence is analyzed. The investigation applies the Haines Index (HI), which indicates the potential for wildfire growth by measuring the stability and dryness of the air. Three simulations have been analyzed: for Last Glacial Maximum (LGM), the mid-Holocene (MH) and present day (MOD) conditions. The results indicate that for present day conditions, the HI is a useful tool to identify areas with high susceptibility for fire occurrence, such as the west coast of the United States and the central part of South America. Analyses for the glacial epoch demonstrated that in respect to MOD conditions, the HI is intensified in Africa and south Asia. It is reduced, however, in Australia, the west coast of North America, Europe and in northern Asia. During the mid-Holocene, the atmospheric conditions were likely more favorable for fire occurrence over North America, sub-Saharan Africa and a large part of Eurasia and South America. In the contrary, Australia, northern Africa and the northern part of South America seem to have been less susceptible to intense fire as compared to current conditions. These findings very closely match paleofire inferences based upon charcoal analyses.

1. Introduction

In recent decades various sectors of society have expressed concern over the indiscriminate use of fire. Impacts of vegetation/wild-land fires are prominent in questions which involve past and future climate change (e.g. Harrison et al., 2007, Lynch et al., 2007, Black et al., 2006, Thonicke et al., 2005, Page et al., 2002). Nevertheless, there exists a lively debate on the importance of anthropogenic and climate forcing in contributing to the ignition of wild-land fires.

Paleoenvironmental studies have shown that forest fires may often be primarily attributed to climate conditions (e.g. Marlon et al., 2008, Markgraf et al., 2007, Whitlock et al., 2006), although human actions could have played a role in terms of ignition source (Huber et al., 2004). According to Bar-Yosef (2002), during the course of human evolution fire was used even in the most remote regions. For southern Southern America, Huber et al. (2004) suggested that, during the Holocene, the impact of the activities of paleo-Indians and the influence of climate on fire occurrence is difficult to separate. Whitlock et al. (2006), however, attributed the change in surface-fire regime during the mid-Holocene in the Argentinian Andes to increased interannual climate variability and the onset or strengthening of ENSO.

The link between paleofire and climate conditions has also been raised by Pierce et al. (2004), Whitlock (2004) and Pyne et al. (1996). They argued that shifts in fire regimes during the Medieval Warm Period and the Little Ice Age were dictated by changing weather conditions and their influence on fuel moisture, ignition conditions and fire behavior. It has also been found that the early decline in biomass burning prior to 1750 occurred in phase with global cooling and despite a rise in human population (Marlon et al., 2008).

Among other environmental implications, fire activity plays an important role in defining the Earth's ecosystems and dominant plant communities (e.g. Pyne et al., 1996, Meyn et al., 2007). As discussed by Ginsberg (1998), forest fires in Brazil and Indonesia during the past two decades may have substantially reduced biodiversity and lead to the occurrence of distinct biological selection. This finding may also be extended to a paleo-perspective. For example, pollen studies in the central region of the Brazilian tropical savanna indicate the presence of charcoal in reconstructions dating back 32,000 yr (Ferraz-Vicentini, 1999), (Salgado-Labouriau and Ferraz-Vicentini, 1994). It should be noted, moreover, that biomass burning is the second largest source of greenhouse gas emission for the atmosphere, which under ancient climate conditions could have played a prominent role for the evolution of the Earth's carbon cycle.

* Corresponding author.
E-mail addresses: fjustino@ufv.br (F. Justino), peltier@atmosp.physics.utoronto.ca (W.R. Peltier), barbosa33@gmail.com (H.A. Barbosa).

0031-0182/$ – see front matter © 2010 Elsevier B.V. All rights reserved.
doi:10.1016/j.palaeo.2010.05.017

This period is characterized by a cold and dry climate as compared to today's climate (Justino and Peltier, 2008, Peltier and Solheim, 2004). These changes, in association with reduced CO_2 concentration, induced modifications of the global vegetation patterns such as: specifically the reduction of the Siberian boreal forest (taiga), an increase in shrub cover in Europe and an increase of the areas of subtropical desert (e.g. Adam and Faure, 1997). It has also been suggested that the tropical rainforest was greatly diminished, especially in West Africa and South America (e.g. Crucifix et al., 2005, Ray and Adams, 2001, Adam and Faure, 1997). One may assume that the replacement of evergreen forest by savanna and grassland, would be more favorable to the occurrence of wildfires due to the amount of fuel available for burning during the dry season.

This highlights the need for a more complete understanding of the interaction between wildfire, climate and the surface land cover, in the sense that such analysis may help to disentangle critical factors for ecosystem dynamics under both present day and previous climate conditions.

The present study is intended to provide further evaluation from a global perspective of the atmospheric conditions associated with fire occurrence for modern, mid-Holocene and LGM intervals by using the Haines Index. This is motivated by the fact that changes in the stability properties of the atmospheric column and in the amount of water vapor in the lower troposphere, need to be carefully evaluated in order to understand the primary causes of fire activity. Although this is an important issue, no previous attempt has been made to systematically investigate, based on a fire index, the link between past atmospheric conditions and the global paleofire records provided by Power et al. (2008).

2. The coupled climate model and the design of the numerical experiments

The coupled atmosphere-ocean-sea-ice model employed in this study is the NCAR-CSM. The atmospheric general circulation component of the model is the low resolution version of CSM 1.4 that incorporates 18 vertical levels in the atmosphere in which the model fields are truncated triangularly at spherical harmonic degree and order 31, which corresponds to 96 by 48 longitude and latitude grid points (Kiehl et al., 1998). The dynamics of the ocean are described on 25 vertical levels on a 3 by 3 degree grid. Additionally, the coupled model includes a sophisticated sea-ice component as well as a simplified representation of land surface processes.

The NCAR-CSM model has been extensively used to simulate the present day climate and no purpose will be served by discussing this in detail herein. In order to investigate the atmospheric susceptibility for wildfires, three model simulations have been analyzed: a present day experiment driven by present day boundary conditions (MOD), a second experiment for the Last Glacial Maximum (LGM, Peltier and Solheim, 2004) and a third simulation focusing on the climate during the mid-Holocene (MH). The MOD (LGM) simulation was run to equilibrium for 2000 (2500) years (Peltier and Solheim, 2004) and the analyses discussed herein are based upon the monthly climatology computed on the last 500 yr of each simulation.

In the LGM simulation, we set the four major boundary conditions that are required for the purpose of such analysis as follows: (I) orbital parameters were fixed to those corresponding to 21,000 yr ago, (II) ice sheet topography and albedo were fixed according to the ICE-4Gmodel (Peltier, 1994), (III) the land-sea mask and paleo sea level were fixed according to the ICE-4G model, and (IV) the concentrations of the radiatively active atmospheric trace gases (CO_2, CH_4 and N_2O) were adjusted based upon estimates from the Vostok ice core. Specifically, these concentrations were taken to be 200 ppmv for CO_2, 400 ppbv for CH_4 and 275 ppbv for N_2O.

The MH simulation is set up according to the requirements of the Paleoclimate Modelling Intercomparison Project (PMIP2). The major difference between the MH and MOD simulations arise from the orbital configuration. The inclusion of the orbital parameters leads to an intensification of the seasonal cycle of the incoming solar radiation at the top of the atmosphere in the Northern Hemisphere and to a decrease in the Southern Hemisphere (Braconnot et al., 2007). This might be taken to imply that the climate during the MH should have been slightly warmer than today in the summer and colder in the winter (Otto-Bliesner et al., 2006).

By comparing the simulated present day climate with the NCEP dataset (Kalnay et al., 1996), we have demonstrated that our MOD simulation predicts lower temperatures for the warmest and coldest months for Eurasia/Scandinavia and the Nordic Seas, whereas warmer conditions over central Europe are also predicted (Justino and Peltier, 2008). Therefore, the CSM model version 1.4 exhibits a cold (warm) bias over high latitudes (sub-tropics) under present day conditions. For LGM climate conditions, Justino and Peltier (2008) presented an extensive inter-comparison between the model results and paleoreconstructions, in which it is found that the simulated LGM climate is in close accord with most recent paleoclimate inferences.

Specifically, the comparison between the simulated temperature anomalies of the warmest month (TWARM, LGM-MOD), and the pollen-based reconstructions reveals that the model reproduces the proxy data satisfactorily over southern Europe/Mediterranean region (Justino and Peltier (2008) their Fig. 2c). It is also clear that the modelled TWARM (LGM-MOD) anomalies are much colder elsewhere than suggested by the palynology. Similar bias is also noted in the temperature of the coldest month (TCOLD, LGM-MOD) anomalies (Justino and Peltier (2008) their Fig. 2d). This discrepancy between model results and reconstructions over high latitudes is strongly related to the presence of the Fennoscandia ice sheet.

Analyses of precipitation amount (Justino and Peltier (2008) their Fig. 2f), in contrast to temperature, demonstrate that the model results and paleoreconstructions are in considerably better agreement in the extratropical region, northward of 50°N. In the subtropical region, however, simulated LGM climate is more arid than suggested by the paleoclimatological reconstructions.

3. Results

3.1. Present day analyses

It has long been recognized that stability characteristics and the amount of water vapor of the atmosphere, are among the major drivers for the initiation and spread of fire (Brotak and Reifsnyder, 1977). Atmospheric moisture directly effects fuel flammability, and associated with other weather characteristics, such as lightning, has indirect consequences for fire behavior. Thunderstorms with strong vertical motion develop as a consequence of convective instability of a moisture of a laden air mass. Lightning associated with such thunderstorms may set wildfires, and the associated winds may have adverse effects on fire behavior (Kennard, 2008).

The instability of the air adjacent to such fire also influences the behavior of the fire, by increasing the vertical dimension of the smoke columns, which induces surface winds due to the thermal gradient between the burning region and the adjacent areas. Consequently, forest fires can create their winds which in turn reinvigorate the atmospheric instability thereby though the action of this positive feedback intensifying the fire activity (Kochtubadha et al., 2001).

Several methods have been developed during the last three decades to assess the atmospheric vulnerability to wildfire occurrence (e.g. the Angstrom Index, the Haines Index, FIRETEC, the McArthur Forest Fire Danger Index and the Canadian Fire Weather Index). These indices are primarily driven by incorporating information concerning atmospheric moisture and temperature. More recently, conceptual models which take into account ecosystem type, and wildfire models

based on balance equations for energy and fuel including detailed combustion physics and data assimilation have also been employed to model wild-land fire risk (Mandel et al., 2008, Meyn et al., 2007, Zhou and Mahalingam, 2001). The latter models, however, incur high computational cost.

Since the Haines Index (HI) was introduced (Haines, 1988), however it has become the primary tool employed by fire managers to assess fire risk. It has also been extensively used by Fire Weather Offices in the United States, Canada and Australia. The HI is a relatively strait way to combine two important atmospheric factors into one simplified model which reasonably indicates the areas more susceptible to fire.

The HI is an index for the estimation of wild-land fire severity (growth potential) based upon environmental lapse rates and moisture (Werth and Werth, 1998, Winkler et al., 2005). The HI is computed from lower-tropospheric and dewpoint temperatures and has three different versions that take into account variations in surface/terrain elevation. For present purposes we will solely employ calculations of HI based upon climate model predictions between the atmospheric levels of 850 and 700 hPa. This is reasonable since the largest HI is found in this layer (Winkler et al., 2005). The Haines Index includes a stability (A) component and a moisture (B) component that are weighted equally. The A component stands for the environmental lapse rate (i.e., the change of temperature with height), whereas the B component is the dewpoint depression for a specific pressure level (Winkler et al., 2005). For both components, the calculated temperature difference (A = T850 hPa − T700 hPa) and water vapor (B = T850 hPa − Td850 hPa) differences are separated into three groups that are assigned a value of 1, 2, or 3 (Table 1). The 850 hPa and 700 hPa atmospheric levels do not experience strong diurnal temperature variation and therefore 850 hPa temperature/moisture are used to compute the HI. This makes it possible to distinguish air masses and thus to locate cold and warm weather systems with highest favorability for growth and spreading of fire.

The A and B components are then summed, and the resulting Haines Index has a range from 2 (very low risk of large or erratic plume-driven behavior) to 6 (high risk). It should be noted that in this study we evaluated the HI based on the temperature values instead of the ordinary Haines values (from 2 to 6). Thus, values smaller than 12 °C indicate a very low potential for large fires, values between 12 and 22 °C suggest a low potential to large fires, and values above 22 °C are associated to moderate and high probability for the occurrence of large fires. This seems justified by the fact that in analyzing temperature, additional information on the atmospheric stability and the amount of water vapor may help to understand the substantially modified climate of the LGM and the MH.

The HI does suffer from a number of drawbacks, however, one example of which is that it does not incorporate information concerning wind, fuel moisture and the characteristics of the surface land cover as input variables.

The performance of the HI as an effective tool for the prediction of wildfire occurrence has been compared to the Canadian Fire Weather Index (FWI) by Mokorić and Kalin (2006). They have shown that the HI is a useful tool for the identification of areas susceptible to large fires. Furthermore, Viegas et al. (1999) demonstrated, by comparing five different fire indices for France, Italy and Portugal that the FWI performed best. Dowdy et al. (2009) noted that the FWI and McArthur Forest Fire Danger Index (FFDI) are similar to each other. These results allows us to conclude that the HI is among the fire models that better reproduced the observed fire risk, due to the similarity between its results and the results proposed by the FWI and FFDI models.

In order to investigate the atmospheric susceptibility for wildfire occurrence under substantially modified climate, it is important to identify a potential model bias in terms of mapped areas of extreme fire risk under present day climate. Fig. 1 shows the seasonal distribution of the Haines index (HI), for both MOD simulation and the NCEP Reanalysis (Kalnay et al., 1996). It appears that the simulated HI very closely matches the calculation of the HI based on the NCEP dataset.

Analyses for DJF (December, January and February) indicate that the atmospheric conditions which would favor fires are very weak northward of 50°N (Fig. 1a,b). Evaluation of the A and B terms, which together characterize the HI, show that for most of this region temperature differences are smaller than 5 °C, indicating weak temperature lapse rates and small vapor pressure deficit (VPD). These conditions are associated with a low probability of large wildfires.

Southward of 50°N, one may highlight the high value of the HI in Australia and Sahelian Africa. Over the sub-Saharan region, the B term (vapor pressure deficit, VPD) is responsible for the high HI, since the contribution of the stability component (A term) is negligible (not shown). In Australia, however, both stability (A) and the moisture (B) terms equally contribute to the magnitude of the HI. This agrees with the highest incidence of observed vegetation fires in these regions during the Southern Hemisphere summer season (Davis and Holmgren, 2001).

Analyses for the Northern Hemisphere spring season (MAM, March–April–May, Fig. 1c,d), demonstrate an intensification of atmospheric conditions favorable to the presence of wildfire, in particular over the Middle-East and South Asia, Western North America, and in the Amazon forest and Brazilian savannas. It should be noted that the Haines Index is even stronger in JJA (June–July–August), than in MAM.

Over the Middle-East, South Asia and North America, the dryness of the atmosphere as reproduced by the difference between the dew point and the air temperature at 850 hPa, plays the key role for the enhancement of the HI. In South America and sub-Saharan Africa, however, the highly unstable atmosphere controls the magnitude of the HI. During the SON period, it could be argued that the atmosphere in general does not provide supportive conditions for the occurrence of large wildfires, except in the southern part of Africa, Australia and

Table 1
Calculation of Haines Index according to terms A and B as function of elevation.

Elevation	Stability (A) component		Moisture (B) component	
	Calculation	Categories	Calculation	Categories
Low (≤1500m)	A = T950 hPa − T850 hPa	A = 1 if <4 °C A = 2 if 4–7 °C A = 3 if ≥8 °C	B = T850 hPa − Td850 hPa	B = 1 if <6 °C B = 2 if 6–9 °C B = 3 if ≥10 °C
Mid (1500–3500 m)	A = T850 hPa − T700 hPa	A = 1 if <6 °C A = 2 if 6–10 °C A = 3 if ≥11 °C	B = T850 hPa − Td850 hPa	B = 1 if <6 °C B = 2 if 6–12 °C B = 3 if ≥13 °C
High (≥3500m)	A = T700 hPa − T500 hPa	A = 1 if <18 °C A = 2 if 18–21 °C A = 3 if ≥22 °C	B = T700 hPa − Td700 hPa	B = 1 if <15 °C B = 2 if 15–20 °C B = 3 if ≥21 °C

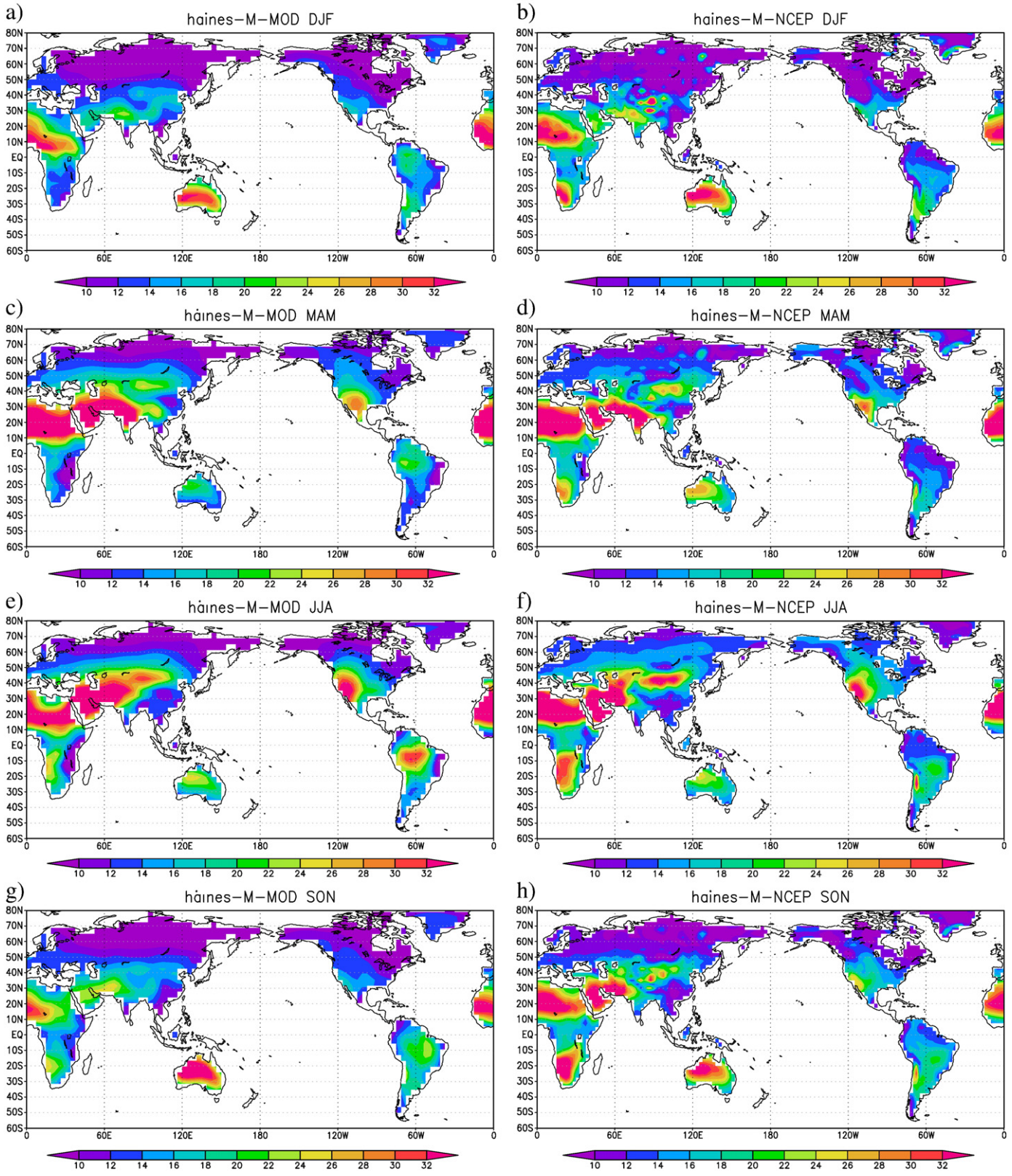

Fig. 1. Haines Index distribution based on MOD simulation a) DJF, c) MAM, e) JJA and g) SON. Similar calculation for the NCEP reanalyses. b) DJF d) MAM, f) JJA and h) SON.

Brazil. This is the most prominent feature in the Haines Index distribution as computed from the NCEP data (Fig. 1g,h).

A further validation of the modelled HI by the MOD simulation is through comparison with the World Fire Atlas (Fig. 2). The World Fire Atlas forms a unique long time series of global fire location and timing. One may note that the higher values of the HI based on the MOD simulation as well as on the NCEP reanalysis, are correctly located in areas of satellite-detected hot spots with brightness temperature

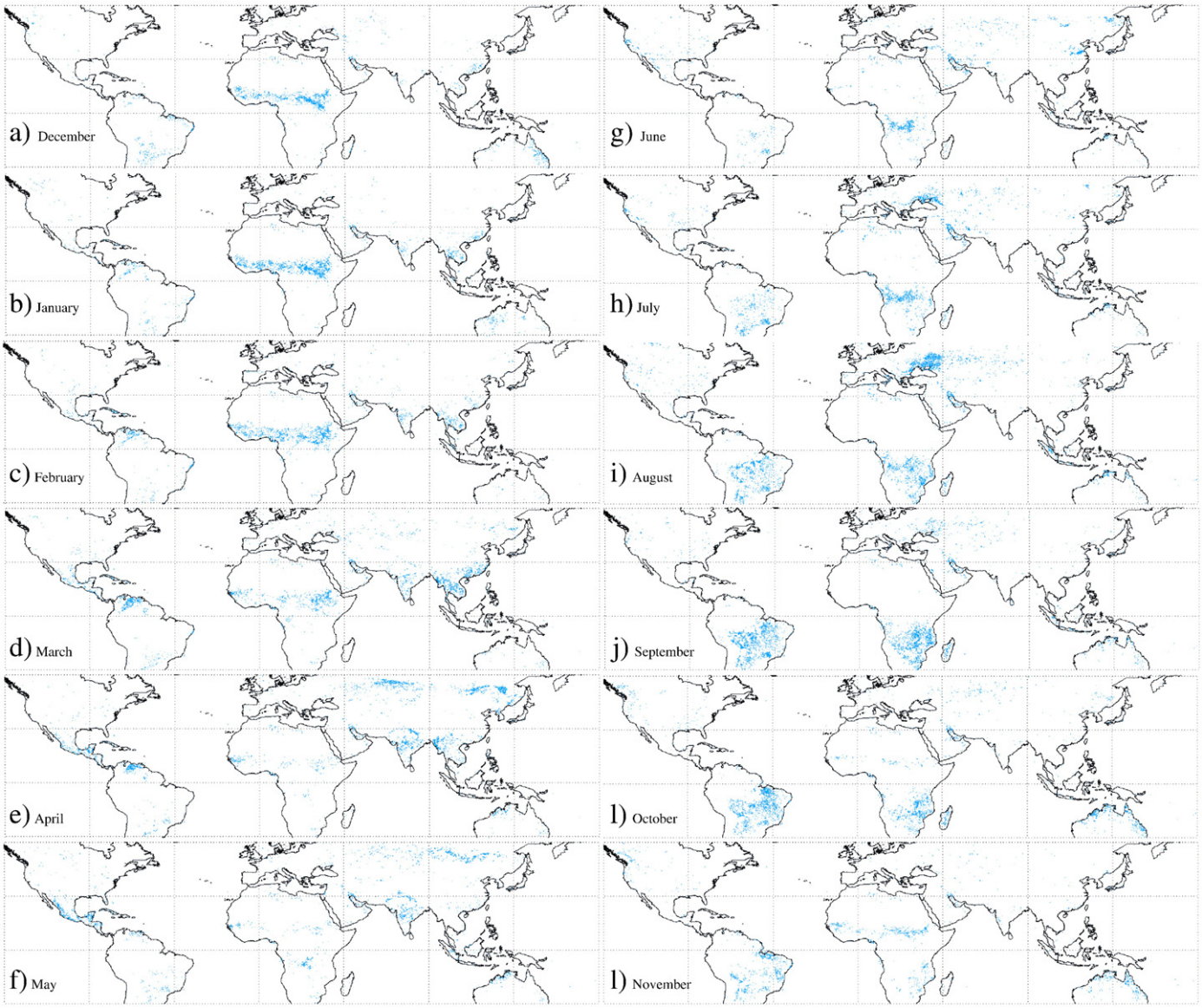

Fig. 2. Satellite-detected hot spots with brightness temperature higher than 308K in the year 2008. Source: http://dup.esrin.esa.int/ionia/wfa/index.asp.

higher than 308K, which indicates fire activity. It should also be noted that Fig. 2 illustrates the hot spots detected during the year 2008. This year experienced moderate fire activity, although there is no strong interannual variability in the areas with recurrent fires.

Fig. 2a, b and c, shows that during the NH winter season wild-land fires are primarily detected in South America, the central part of Africa, southern Asia and Australia. This should be compared with values larger than 28 °C as shown in Fig. 1a and b, which indicates high probability of fire according inferences based upon the HI.

The onset of the rainy season in Africa and Australia in MAM reduces the fire activity over these regions (Fig. 2d,e,f). During these months fires are predominantly observed in southern North America, central America, northern South America, southern Asia and Russia. It is interesting to note that the HI is able to account for seasonal changes in satellite based-wildfires by increasing the environmental risk, in particular in southern Asia and North America (Fig. 1c,d). However, the HI exhibits unrealistically high fire risk over the Sahara desert despite the low fuel availability associated with the scarcity of vegetation.

During JJA dry conditions dominate in most parts of the Southern Hemisphere. This season exhibits the largest number of hot spots globally (Fig. 2g,h,i), primarily in Brazil and sub-Saharan Africa, and parts of Eurasia. This corresponds closely with highly favorable conditions for wildfire development as implied by the HI (Fig. 1e). Similar results may be obtained for SON conditions. This initial evaluation of model performance in simulating areas with large wildfire ignition probability, and their agreement with the global fire distribution, demonstrate that the Haines Index is well suited to the investigation of areas susceptible to fire occurrence from a global perspective. Again, one should note that the HI refers to climatic conditions only and ignores any influence of available vegetation in providing the fuel to burn.

3.2. Last Glacial Maximum analyses

In order to investigate the atmospheric susceptibility to wildfire ignition during the Last Glacial Maximum, the HI is computed from the LGM simulation output. Fig. 3 shows the anomalies between the A

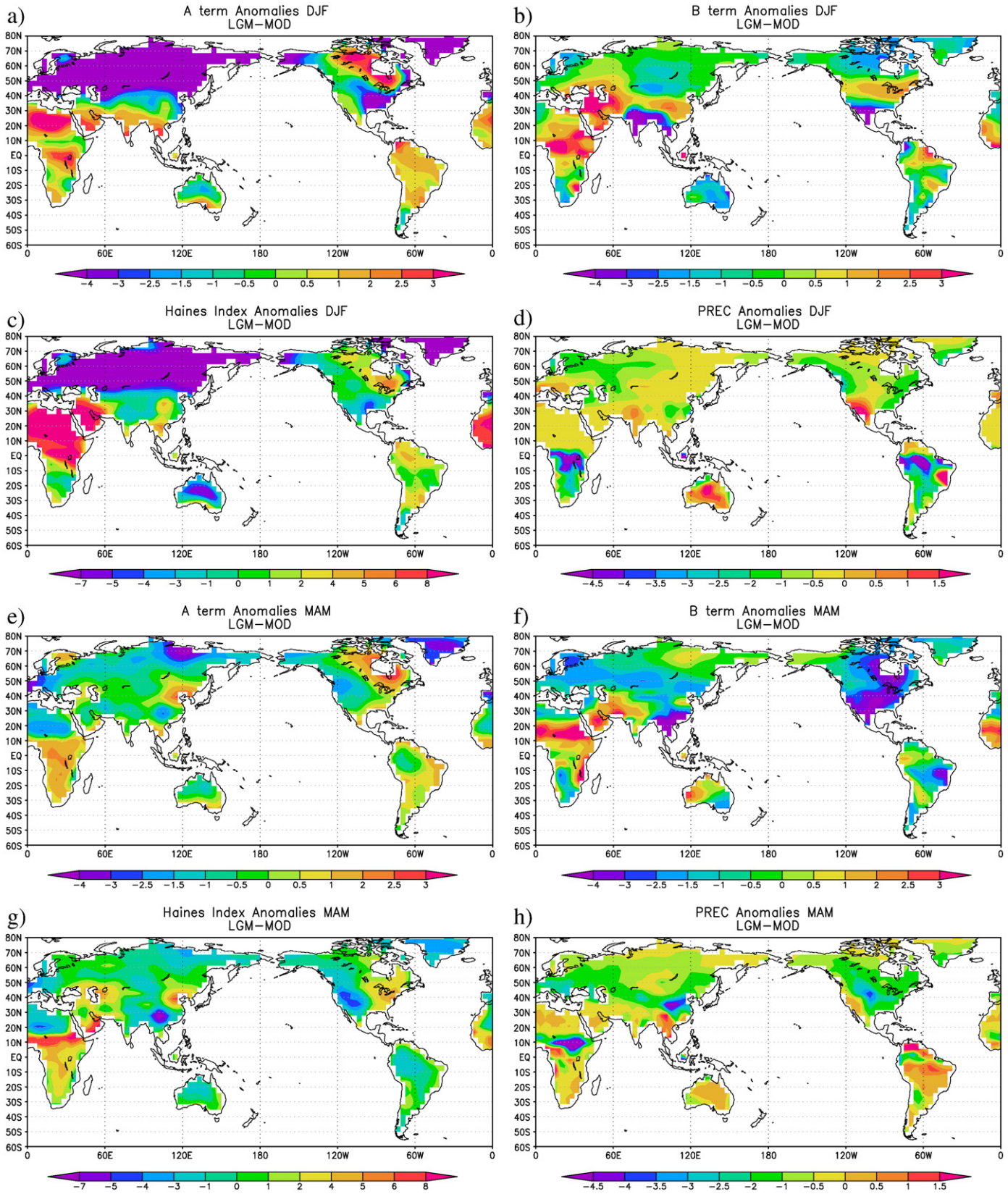

Fig. 3. Anomalies of the Haines Index and its components between LGM and MOD simulations (°C). a) A term in DJF, b) B term in DJF, c) Haines Index in DJF and d) precipitation anomalies between LGM and MOD simulations in DJF (mm/day). Similar to a, b, c, and d but for MAM (°C). e) A term, f) B term, g) Haines Index and h) precipitation anomalies between LGM and MOD simulations in MAM (mm/day).

and B terms for the LGM and MOD simulations. It should be noted that during the LGM, the land surfaces in North America and Scandinavia were covered by the Laurentide and Fennoscandian ice sheets. Therefore, no fire activity would be expected in these areas. Fig. 3a and b in general demonstrates that during the LGM, in the boreal winter season (DJF), there exists an intensification of the A and B

terms in the tropical regions, except in Australia, when compared to present day conditions. This reveals that the inclusion of glacial boundary conditions in the model simulations induces a more unstable atmospheric layer – through an increase of the lapse rate – between 850 and 700 hPa. This has also been suggested by Wille et al. (2000), who argued for a modified lapse rate during the ice age that would significantly steepen the temperature gradient between lowlands and highlands.

In addition, one may note an increase in the vapor pressure deficit at 850 hPa (B term) in Africa, the Middle-East, North America and the Amazon region (Fig. 3b). This is primarily due to reduced evaporation as a result of the arid LGM climate.

The sum of the anomalies of the A and B terms, which characterizes the difference of the Haines Index between modern and LGM conditions is shown in Fig. 3c. Over Eurasia and Australia a reduction in the atmospheric susceptibility to wildfire which in the former region is associated with stronger atmospheric stability during the LGM; in Australia, however, the stability and moisture terms contribute equally.

In the northern and sub-Saharan Africa as well as over northern South America, the Haines Index anomalies suggest an intensification of the environmental conditions favorable to fire occurrence. This is supported by charcoal records in the tropical latitudes of South America and Africa which show higher-than-present fire activity from 19,000 to 17,000 BP (Power et al., 2008). Moreover, increased atmospheric susceptibility to fire activity as predicted to occur in southeast Asia is also supported by the charcoal data. Although positive anomalies of the Haines Index are simulated in Africa there is no evidence of more fires having occurred in that region than occur in the present. Past fire may be detected by measuring the incomplete products of combustion, usually from biomass burning, preserved in lake, swamp, and marine sedimentary sequences (Jones et al., 1997).

To further evaluate the atmospheric conditions which may help to initiate fire activity, we have analyzed seasonal precipitation anomalies. Reduction in the precipitation rate is associated with decreased vegetation wetness which may increase the flammability of the combustible material and lead to fire ignition. It may be noted that areas with positive (negative) anomalies of HI (Fig. 3c,d) are in general closely linked to reduced (increased) precipitation.

Climate conditions in MAM, the NH are characterized by a decrease in both the stability and moisture components of the HI, as compared to DJF (Fig. 2e,f). In regard to precipitation changes, it has been demonstrated that most of the NH experienced reduced rainfall during the LGM interval compared to the present (Fig. 3h). In addition to this reduction in precipitation the presence of huge ice sheets and low temperatures were clearly not favorable for fire occurrence. In contrast, increased precipitation in southeast Asia and South America, although regionally highly variable, still would result in atmospheric conditions promoting fire occurrence during the LGM (Fig. 3g).

Turning to the potential fire activity during the boreal summer season (JJA), which globally and under today's conditions result in the highest number of wild-land fires, simulations produced an intensification of the atmospheric lapse rate, i.e. the A term of the HI, in Asia and sub-Saharan Africa of up to 3 °C (Fig. 4a). The second component of the HI, the dewpoint depression (B term, Fig. 4b), shows, in comparison with the A term, that the inclusion of LGM conditions may have reduced the vulnerability of the land system to fires.

Average summertime Haines Index anomalies match very closely the anomalies of the A term. It may be concluded that during the Last Glacial Maximum, the atmospheric susceptibility for fire activity during the NH summer season was very likely reduced, in particular in the American continent (Fig. 4c). In addition, during the summer season, vegetation wetness southward of 50°N was probably higher due to increased precipitation, which may reduce the flammability of combustible material (Fig. 4d). The evaluation of the A and B terms for the boreal autumn (SON, Fig 4g,h) exhibits many similarities with the distribution predicted to occur in the winter season (Fig 3a,b).

3.3. Mid-Holocene analyses

Several studies highlight the mid-Holocene (7000 to 5000 BP) as a period of particularly profound change (e.g. Otto-Bliesner et al., 2006, Steig, 1999). During this interval, land air temperatures appear to have increased from LGM conditions, however annually averaged temperatures were lower across much of the globe in comparison with present day climate. In the northern hemisphere the analyses are more complicated, since the climate is expected to have been warmer than today during the mid-Holocene in summer and colder in winter (Otto-Bliesner et al., 2006).

In terms of fire regime, Power et al. (2008) show that during the mid-Holocene (MH), 43% of all records show less-than-present fires. Regional summaries show greater-than-present fire in Central and South America, less-than-present fire in eastern North America, and heterogeneous conditions similar to modern across Europe. Pollen evidence indicates that grassland and xerophytic woodland/shrubs expanded during the mid-Holocene in areas of northern Africa which are characterized by desert today during the mid-Holocene (Jolly et al., 1998). This may suggest a wetter climate in these areas (Hoelzmann et al., 1998).

In the following the atmospheric predisposition to wildfires is discussed for the mid-Holocene (MH) period. Compared to anomalies of the A and B terms for the LGM interval, the MH anomalies show more homogeneity in the global distribution throughout the year (Figs. 5, 6). This is also suggested by the smaller range of changes of the A and B terms in respect to their LGM counterparts (Figs. 3, 4). In DJF the main patterns associated with the MH are the positive anomalies of the moisture (B) term in central Africa, southeastern Asia, United States and the northern South America, which leads to positive Haines Index anomalies, except in South America (Fig. 5c) due to the negative anomalies of the A term (Fig. 5a). It should be stressed that the marked drop in precipitation (Fig. 5d), as predicted to occur during the MH corroborates the increase in the environmental flammability.

As compared to current conditions, analyses for MAM demonstrate an intensification of the atmospheric lapse rate (Fig. 5e), but more humid conditions as represented by reduced dewpoint depression (Fig. 5f). By combining these anomalies, an increase in the Haines Index over North America, northeast Asia, Europe and part of Africa is inferred (Fig. 5g). It is interesting to note, furthermore, that the areas with positive anomalies of the HI are dominated by a deficit in precipitation which implies more arid conditions (Fig. 5h).

Analyses of the NH summer, show that a tendency toward more vigorous updrafts, as well as dryer conditions appears in Asia, and over both North and South America (Fig. 6a,b). The Haines Index also shows increased atmospheric susceptibility for fire occurrence in central Asia and North America (Fig. 6c). It should also be noted that, according to our analyses, strong negative anomalies of the HI appear in Africa, consistent with the higher precipitation (Fig. 6d). Changes in SON are smaller and seem not to modify the fire risk in comparison to modern conditions.

4. Harmonic analysis

In order to study the seasonal spatial variability of the HI, we have applied harmonic analyses. As discussed by Aslan et al. (1997), the Fourier transformation or harmonic analysis decomposes a time-dependent periodic phenomenon into a series of sinusoidal functions, each defined by unique values of amplitude and phase. The proportion of the variance in the original time-series data set accounted for by each term of the harmonic analysis can also be simply calculated (Jakubauskas et al., 2001).

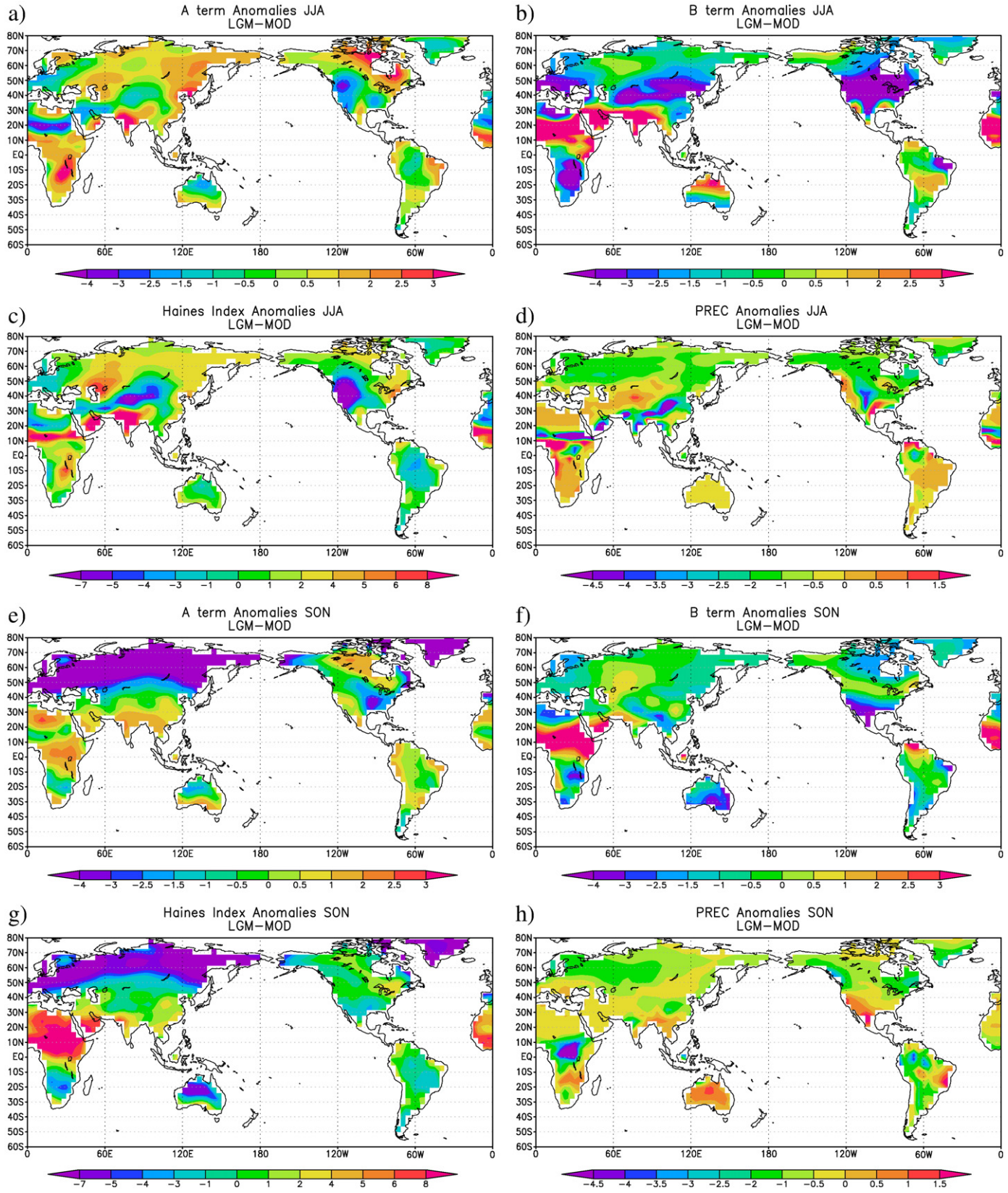

Fig. 4. As Fig. 3 but for JJA and SON.

The lowest order harmonics of meteorological parameters capture long timescale effects, while higher order harmonics show the effects of short term fluctuations (Justino et al., 2010). The phase angle can be used to determine the time when the maximum or minimum of a given harmonic occurs. The harmonic analysis is, therefore, a useful tool to characterize different climate regimes and transition regions

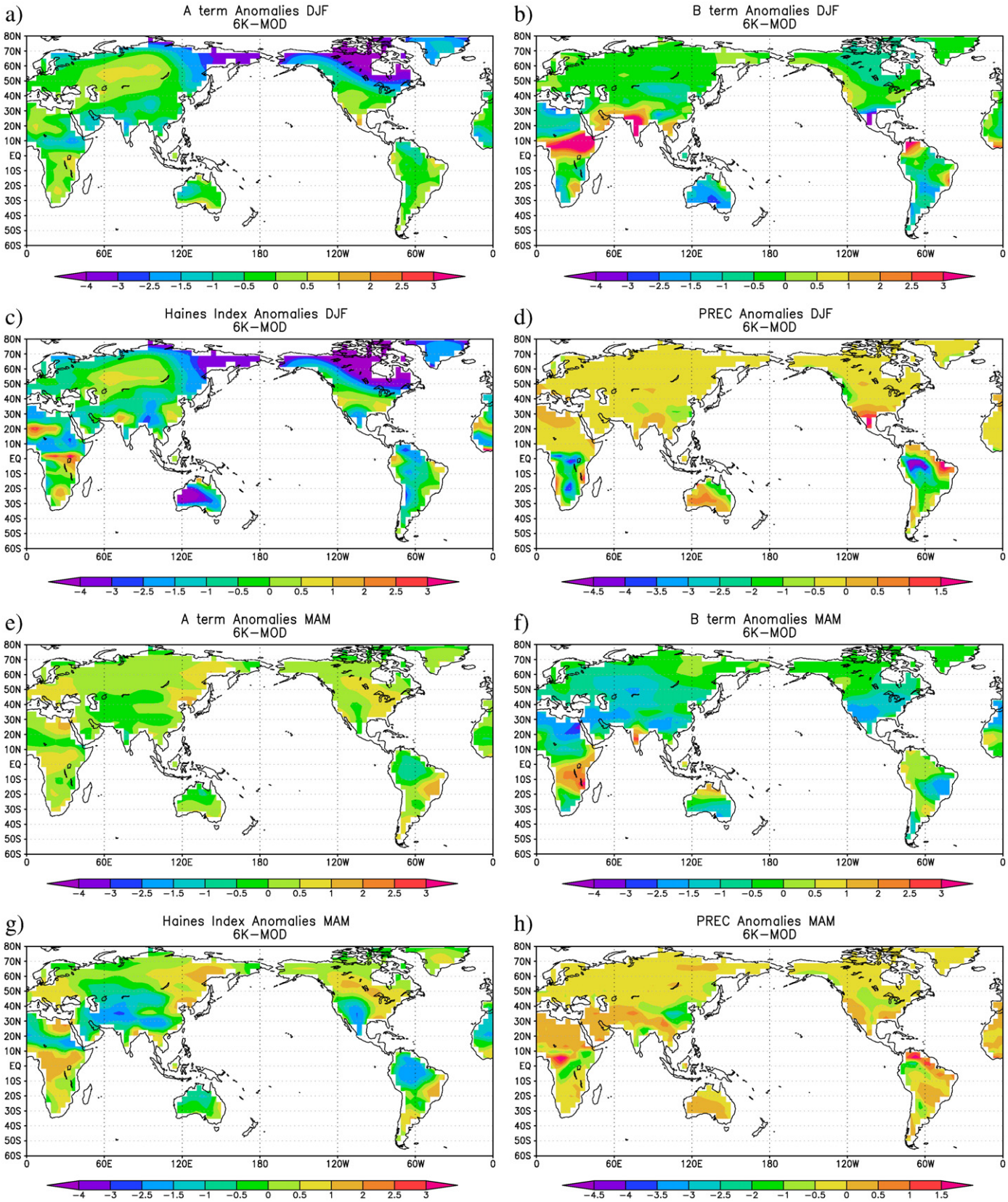

Fig. 5. As Fig. 3 but for mid-Holocene.

with distinct land characteristics. Moreover, the advantage of using this mathematical approach is associated with the possibility of identifying dominant climate features in the space-time domain. It is important to note that investigations based upon area averaged time series are embedded with small and large scale processes dictated by distinct periodicity, which in turn may cancel out regional climatic

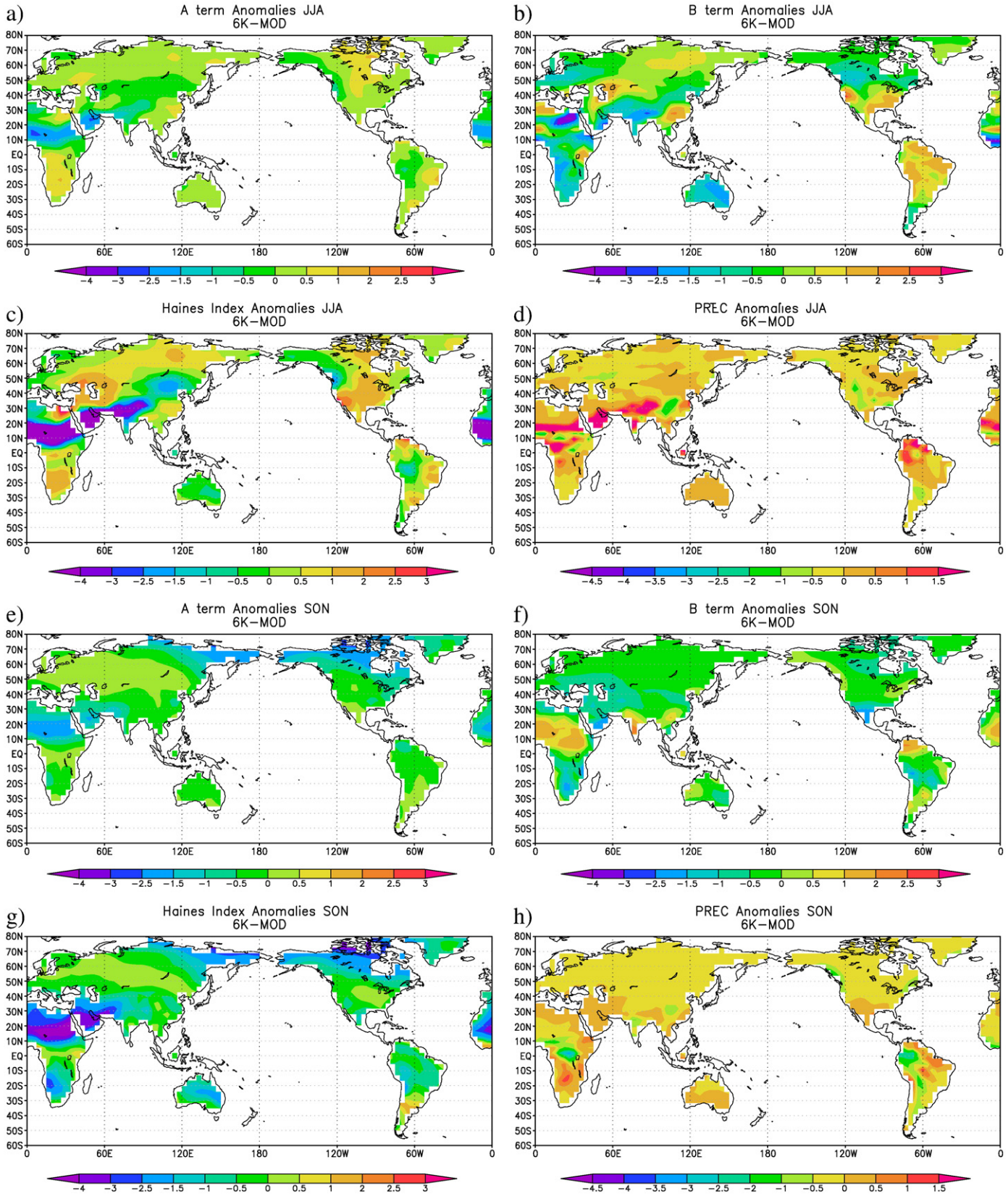

Fig. 6. As Fig. 4 but for mid-Holocene.

signals in the space-time domain. Harmonic analysis is based on the decomposition of the original time series into a series of trigonometric functions (Wilks, 1995), as:

$$y_t = \overline{y} + \sum_{j=1}^{N} C_j \cos(\omega_j t - \varphi_j) \quad (1)$$

in which y_t is the value at time t, $\overline{y}$ stands for the arithmetic mean, Cj is the amplitude of harmonics 'j', t is the time, ω_j is the frequency, φ_j is the phase angle, and N represents the number of observations. The amplitude is calculated from

$$C_j = \sqrt{A_j^2 + B_j^2}. \quad (2)$$

In which A_j and B_j are given by:

$$A_j = \frac{2}{N}\sum_{t=1}^{N} y_t \cos\left(\frac{2\pi t}{N}\right); \quad B_j = \frac{2}{N}\sum_{t=1}^{N} y_t \sin\left(\frac{2\pi t}{N}\right).$$

The phase angle is dependent on the A_j value and may be computed as:

$$\varphi_j = \begin{cases} \tan^{-1}\dfrac{B_j}{A_j} A_j > 0 \\ \tan^{-1}\dfrac{B_j}{A_j} \pm \pi \ \text{ or } \ \pm 180^{\circ} A_j < 0 \\ \dfrac{\pi}{2} \ \text{ or } \ 90^{\circ} A_j = 0. \end{cases} \quad (3)$$

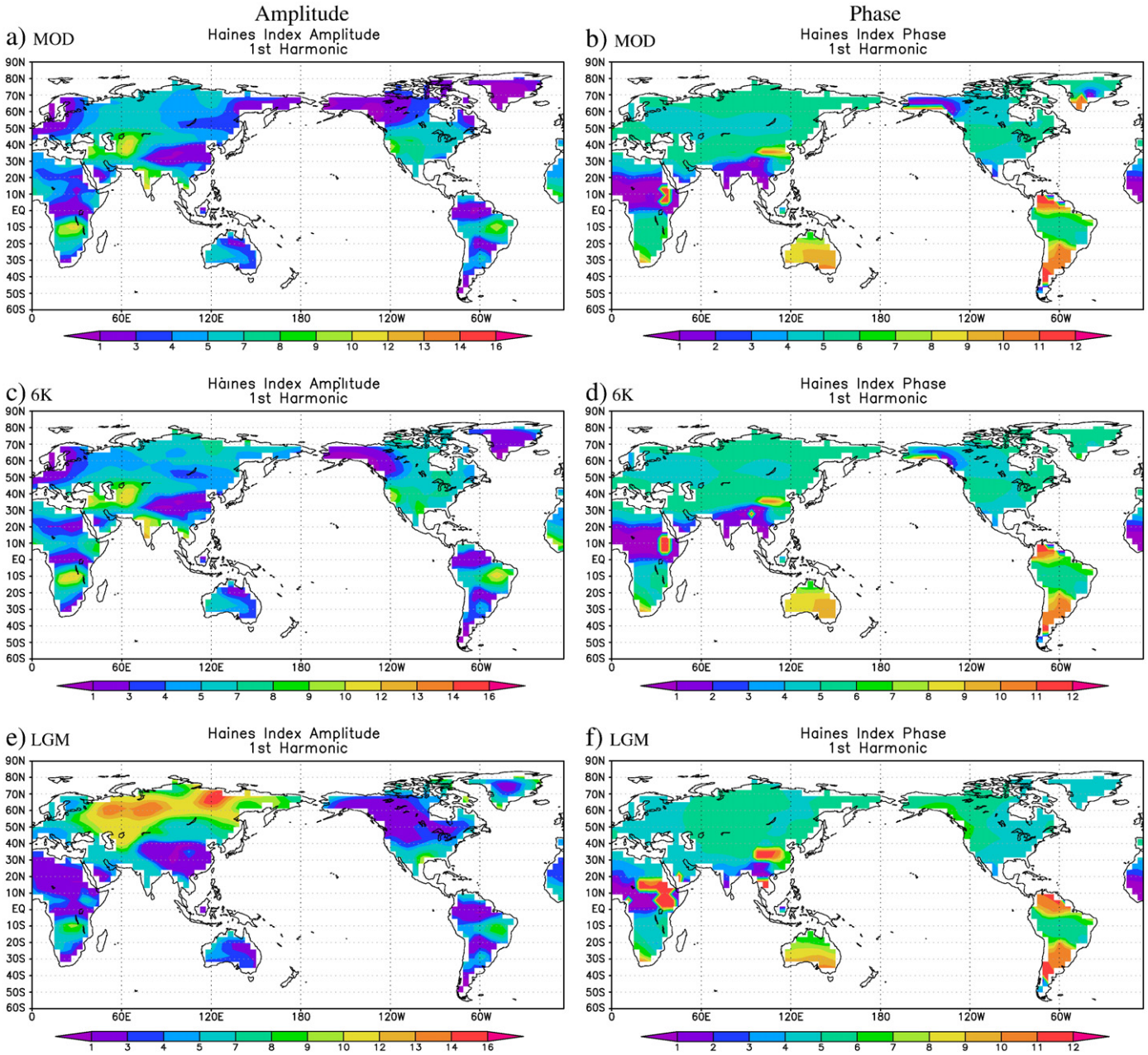

Fig. 7. Amplitude of the 1st harmonic for MOD (a), MH (b) and LGM (c) simulations. (d), (e) and (f) are the phase angles for MOD, MH and LGM simulations.

Contribution by individual harmonics (j) to total variance of the time series is given by $j = \frac{C_j^2}{2s^2}$, where s is the variance of the time series.

The potential of the harmonic analysis approach in the classification of eco-climatic zones has been discussed by Azzali and Menenti (2001). It has also been demonstrated that fundamental characteristics related to the inter- and intra-seasonal characteristics of dynamic ecosystems can be identified by harmonic analysis.

Fig. 7 shows the amplitude and phase of the first harmonic for the MOD, MH and LGM simulations. The amplitude of the annual harmonic shows the differences between the highest and the lowest values of the HI throughout the year. Larger amplitudes of the HI will be associated with a dominant wildfire season. For modern conditions large seasonal differences in the magnitude of the HI are located in central South America, North America, South Africa and southeast Asia (Fig. 7a). These characteristics are also shared by the MH simulation. Over South America, however, the amplitude during the MH interval was higher than for present conditions. Higher (lower) amplitude of the first harmonic indicates stronger (weaker) contrast between the dry and humid seasons and, therefore increased (reduced) risk of wildfire.

Based on the LGM results (Fig. 7c), the northern part of Eurasia was characterized by well defined seasonal cycle. One may not assume, however, that more fire should be expected, since during the LGM the cold climate and presence of snow cover would have reduced the vegetation flammability and ignition.

Analyses of the phase angle, which identify the month with highest fire probability, demonstrated that there are no substantial modifications in the period of fire occurrence among these three periods. Under MOD, MH and LGM conditions, the phase angle shows that in the central part of South America intense fires are expected to occur between June and August, while in the southern and northern regions the fires primarily occur from October to January. Fire activity peaks in the NH during spring/summer which agrees very closely with the observed current fire activity.

5. Concluding remarks

Despite advances in the identification of paleofire abundance through analysis of charcoal particles, studies evaluating the association of climate patterns with fire occurrence are still scarce. By conducting multi-century climate simulations with different climate forcing parameters characteristic of the Last Glacial Maximum (LGM), mid-Holocene (MH) and present (MOD), we have investigated the environmental susceptibility to fire occurrence during these periods. The results presented here indicate that for present day conditions, the Haines Index (HI) is a useful tool for the identification of areas with high probability for large fires, such as the western United States and the central part of South America.

Analyses for the glacial maximum interval demonstrated that under glacial boundary conditions, the atmospheric layer is more unstable due to a strengthening of the lapse rate — between 850 and 700 hPa. There also exists an increase in the vapor pressure deficit at this time which is higher compared to present day. It should be noted that these findings depend upon the season. Therefore, we show in Fig. 8a,b the annual mean anomalies of the Haines Index that may be compared to the charcoal distribution provided by Power et al. (2008). Compared to MOD conditions, for the Last Glacial Maximum the HI is intensified in Africa and South Asia but reduced in Australia, the west coast of North America, Europe, and over northern Asia.

Analyses for the mid-Holocene revealed that in North America, sub-Saharan Africa, parts of Eurasia and South America, the environmental conditions were more favorable to fire occurrence. Australia, northern Africa and the northern part of South America, in contrast, seem to have been less susceptible to large fire compared to current conditions.

Comparison of Fig. 8a and b reveals that the magnitude of the HI anomalies are larger for LGM than for MH conditions. However, the Earth system seems to have experienced a higher number of wildfires during the MH than during the LGM. According to Power et al. (2008), charcoal records for eastern and western North America and western Europe indicate less fire activity than present from 21,000 to 9000 calendar years before present (BP). In southern South America, there was less fire than today between 21,000 and 11,000 cal yr BP. In contrast, tropical Indochina and Australia had more fires from 18,000 to 13,000 cal yr BP. Records of fires from tropical South and Central America indicate a brief period of greater-than-present fire between 19,000 and 17,000 cal yr BP, followed by a period of less fire than today until after 10,000 cal yr BP. During the Holocene, with the exception of eastern North America and eastern Asia from 8000 to 3000 cal yr BP, Indonesia and Australia from 11,000 to 4000 cal yr BP, and southern South America from 6000 to 3000 cal yr BP fire activity was less than present.

It is known that the majority of present day fires have an anthropogenic origin. However, the results presented in this paper are entirely independent of human action and are based only upon the atmospheric vulnerability to the occurrence of fire. Moreover, fires of anthropological origin are often directly related to hunting and agroforestry activities. Since the human presence during the LGM was scarce less human induced-fire should also be expected. But independently of the ignition source the climatic conditions need to be right to promote fire.

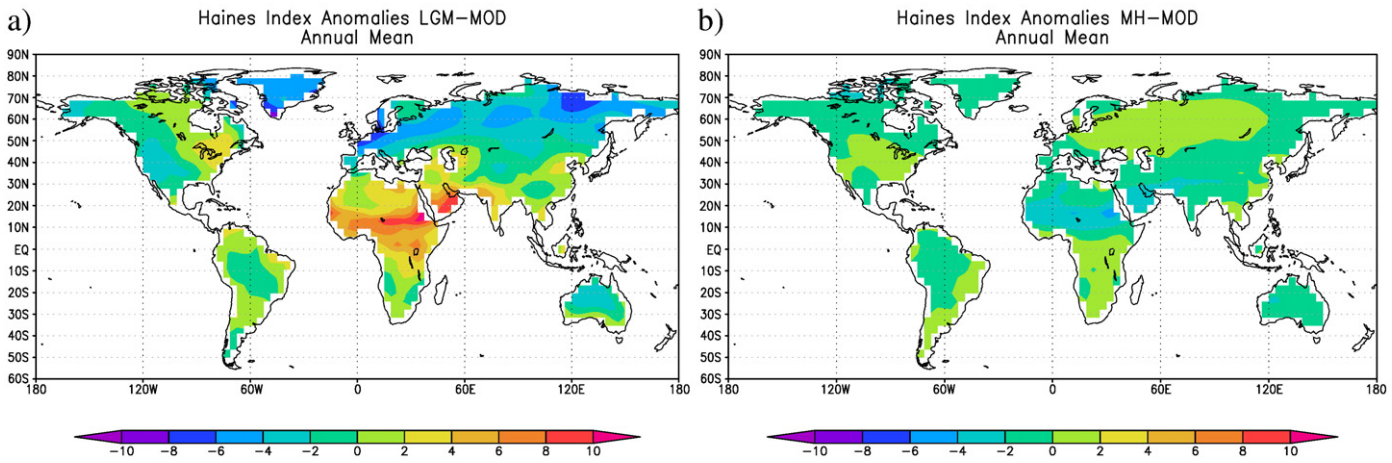

Fig. 8. Global anomalies of the Haines Index in respect to present day conditions. a) LGM at 21000 cal yr BP and b) mid-Holocene at 6000 cal yr BP.

Acknowledgments

Support for this research has been provided through Fundação de Amparo à Pesquisa do Estado de Minas Gerais - FAPEMIG (proj. CRA-PPM-00212-08), and through the Brazilian National Research Council (CNPq) project 479007/2007-1.

References

Adam, J., Faure, H., 1997. Palaeovegetation maps of the Earth during the Last Glacial Maximum, and the early and mid Holocene: an aid to archaeological research. Journal of Archaeological Science 24, 623–647.

Aslan, Z., cu, D.O., Kartal, S., 1997. Harmonic analysis of precipitation, pressure and temperature over Turkey. Il Nuovo cimento 20, 595–605.

Azzali, S., Menenti, M., 2001. Mapping vegetation–soil–climate complexes in Southern Africa using temporal Fourier analysis of Noaa-Avhrr Ndvi data. International Journal of Remote Sensing 21, 973–996.

Bar-Yosef, O., 2002. The upper paleolithic revolution. Annual Review of Antropology 31, 363–393.

Black, M., Mooney, S., Martin, H., 2006. Proposed bio-geological and chemical based terminology for fire-altered plant matter. Quaternary Science Reviews 25.

Braconnot, P., Otto-Bliesner, B., Harrison, S., Joussaume, S., Peterchmitt, J.-Y., Abe-Ouchi, A., Crucifix, M., Driesschaert, E., Fichefet, T., Hewitt, C.D., Kageyama, M., Kitoh, A., Lan, A., Loutre, M.-F., Marti, O., Merkel, U., Ramstein, G., Valdes, P., Weber, S.L., Yu, Y., Zhao, Y., 2007. Results of PMIP2 coupled simulations of the Mid-Holocene and Last Glacial Maximum, Part 1: experiments and large-scale features. Climate of the Past 3, 261–277 URL http://www.clim-past.net/3/261/2007/.

Brotak, T.L., Reifsnyder, W.E., 1977. Predicting major wildfire occurrence. Fire Management Notes 38, 1977.

Crucifix, M., Hewitt, C.D., Betts, R.A., 2005. Pre-industrial-potential and Last Glacial Maximum global vegetation simulated with a coupled climate-biosphere model: diagnosis of bioclimatic relationships. Global and Planetary Change. doi:10.1016/j.gloplach.2004.10.001.

Davis, R., Holmgren, P., 2001. Global forest fire assessment 1990–2000. Technical report, Food and Agricultural Organization of the United Nations.

Dowdy, A.J., Mills, G.A., Finkele, K., de Groot, W., 2009. Australian fire weather as represented by the McArthur Forest Fire Danger Index and the Canadian Forest Fire Weather Index. Technical report, The Centre for Australian Weather and Climate Research.

Ferraz-Vicentini, K. R., 1999: História do Fogo no Cerrado: uma análise palinológica. Ph. D. thesis, Universidade de Brasilia.

Ginsberg, J.R., 1998. Perspectives on wildfire in the humid tropics. Conservation Biology 12, 942–943.

Haines, D.A., 1988. A lower atmosphere severity index for wildland fires. National Weather Digest 13, 23–27.

Harrison, S.P., Power, M., Bond, W., 2007. Palaeofires and the Earth system. iLEAPS Newsletter 3, 18–20.

Hoelzmann, P., Jolly, D., Harrison, S.P., Laarif, F., Bonnefille, R., Pachur, H.-J., TEMPO, 1998. Mid-Holocene land-surface conditions in northern Africa and the Arabian Peninsula: a data set for the analysis of biogeophysical feedbacks in the climate system. Global Biogeochemical Cycles 12, 35–51.

Huber, U.M., Markgraf, V., Schabitz, F., 2004. Geographical and temporal trends in Late Quaternary fire histories of Fuego-Patagonia, South America. Quaternary Science Reviews 23, 1079–1097.

Jakubauskas, M.E., Legates, D., Kastens, J.H., 2001. Harmonic analysis of time-series AVHRR NDVI data. Photogrammetric engineering and remote sensing 67, 461–470.

Jolly, D., Harrison, S.P., Damnatiand, B., Bonnefille, R., 1998. Simulated climate and biomes of Africa during the Late Quaternary: comparison with pollen and lake status data. Quaternary Science Reviews 17, 629–657.

Jones, T.P., Chaloner, W.G., Kuhlbusch, T.A.J., 1997. Sediment records of biomass burning and global change. Proposed Bio-Geological and Chemical Based Terminology for Fire-Altered Plant Matter. Springer-Verlag, pp. 9–22. chapter.

Justino, F., Peltier, W.R., 2008. Climate anomalies induced by the Arctic and Antarctic oscillations: Glacial Maximum and present-day perspectives. Journal of Climate 21, 459–475.

Justino, F., Setzer, A., Bracegirdle, T.J., Mendes, D., Grimm, A., Dechiche, G., Schaefer, C.E. G.R., 2010. Harmonic analysis of climatological temperature over Antarctica: present day and greenhouse warming perspectives. International Journal of Climatology. doi:10.1002/joc.2090.

Kalnay, E., Kanamitsu, M., Kistler, R., Collins, W., Deaven, D., Gandin, L., Iredell, M., Saha, S., White, G., Woolen, J., Zhu, Y., Chelliah, M., Ebisuzaki, W., Higgins, W., Janowiak, J., Mo, K.C., Ropelewski, C., Wang, J., Leetma, A., Reynolds, R., Jenne, R., Joseph, D., 1996. The NCEP-NCAR 40 year reanalysis project. Bulletin of the American Meteorological Society 77, 437–471.

Kennard, D., 2008. Encyclopedia of Southern Fire Science. USDA Forest Service, Southern Research Station. URL http://fire.forestencyclopedia.net/p/p358.

Kiehl, J.T., Hack, J., Bonan, G., Boville, B., Williamson, D., Rasch, P., 1998. The National Center for Atmospheric Research Community Climate Model: CCM3. Journal of Climate 11, 1131–1149.

Kochtubadha, B., Flanniigan, M.D., Gyakyum, J.R., Stewart, R.E., 2001. The influence of atmospheric instability on fire behavior in Northwest Territories, Canada. Fourth Symposium on fire and forest Meteorology meeting. American Meteorological Society.

Lynch, A.H., Beringer, J., Kershaw, P., Marshall, A., Mooney, S., Tapper, N., Turney, C., Kaars, S.V.D., 2007. Using the paleorecord to evaluate climate and fire interactions in Australia. Annual Review of Earth and Planetary Sciences. doi:10.1146/annurev.earth.35.092006.145055.

Mandel, J., Bennethum, L.S., Beezley, J.D., Coen, J.L., Douglas, C.C., Kim, M., Vodacek, A., 2008. A wildland fire model with data assimilation. Mathematics and Computers in Simulation 79, 584–606.

Markgraf, V., Whitlock, C., Haberle, S., 2007. Vegetation and fire history during the last 18,000 cal yr B.P. in Southern Patagonia: Mallin Pollux, Coyhaique, Province Aisen (45° 41 30 S, 71° 50 30 W, 640 m elevation). Palaeogeography, Palaeoclimatology, Palaeoecology. doi:10.1016/j.palaeo.2007.07.008l.

Marlon, J.R., Bartlein, P.J., Carcaillet, C., Gavin, D.G., Harrison, S.P., Higuera, P.E., Joos, F., Power, M.J., Prentice, I.C., 2008. Climate and human influences on global biomass burning over the past two millennia. Nature Geoscience 1, 697–702.

Meyn, A., White, P.S., Buhk, C., Jentsch, A., 2007. Environmental drivers of large, infrequent wildfires: the emerging conceptual model. Progress in Physical Geography 31, 287–312.

Mokorić, M., Kalin, L., 2006. Evaluation of meteorological index for forest fire protection in Croatia. Forest Ecology and Management.

Otto-Bliesner, B.L., Brady, E., Clauzet, G., Tomas, S.L.R., Kothavala, Z., 2006. Last Glacial Maximum and Holocene climate in CCSM3. J. Clim. 19, 2526–2544.

Page, S.E., Siegert, F., Rieley, J.O., Boehm, H.-D.V., Jaya, A., Limin, S., 2002. The amount of carbon released from peat and forest fires in Indonesia during 1997. Nature 420, 61–65.

Peltier, W., 1994. Ice age paleotopography. Science 265, 195–201.

Peltier, W., Solheim, L., 2004. The climate of the Earth at Last Glacial Maximum: statistical equilibrium state and a mode of internal variability. Quaternary Science Reviews 335–357.

Pierce, J.L., Meyer, A.G., Jull, A.J.T., 2004. Fire-induced erosion and millennial-scale climate change in northern ponderosa pine forests. Nature 432, 87–90.

Power, M.J., Marlon, J., Ortiz, N., Bartlein, P.J., Harrison, S.P., Mayle, F.E., Ballouche, A., Bradshaw, R.H.W., Carcaillet, C., Cordova, C., Mooney, S., Moreno, P.I., Prentice, I.C., Thonicke, K., Tinner, W., Whitlock, C., Zhang, Y., Zhao, Y., Ali, A.A., Anderson, R.S., Beer, R., Behling, H., Briles, C., Brown, K.J., Brunelle, A., Bush, M., Camill, P., Chu, G.Q., Clark, J., Colombaroli, D., Connor, S., Daniau, A.-L., Daniels, M., Dodson, J., Doughty, E., Edwards, M.E., Finsinger, W., Foster, D., Frechette, J., Gaillard, M.-J., Gavin, D.G., Gobet, E., Haberle, S., Hallett, D.J., Higuera, P., Hope, G., Horn, S., Inoue, J., Kaltenrieder, P., Kennedy, L., Kong, Z.C., Larsen, C., Long, C.J., Lynch, J., Lynch, E.A., McGlone, M., Meeks, S., Mensing, S., Meyer, G., Minckley, T., Mohr, J., Nelson, D.M., New, J., Newnham, R., Noti, R., Oswald, W., Pierce, J., Richard, P.J.H., Rowe, C., ni, M.F.S.G., Shuman, B.N., Takahara, H., Toney, J., Turney, C., Urrego-Sanchez, D.H., Umbanhowar, C., Vandergoes, M., Vanniere, B., Vescovi, E., Walsh, M., Wang, X., Williams, N., Wilmshurst, J., Zhang, J.H., 2008. Changes in fire regimes since the Last Glacial Maximum: an assessment based on a global synthesis and analysis of charcoal data. Climate Dynamics. doi:10.1007/s00382-007-0334-x.

Pyne, S.J., Andrews, P.L., Laven, R.D., 1996. Introduction to wildland fire. Wiley.

Ray, N., Adams, J., 2001. A gis-based vegetation map of the world at the Last Glacial Maximum (25,000–15,000 bp). Internet Archaeology 11, 1–44.

Salgado-Labouriau, M.L., Ferraz-Vicentini, K.R., 1994. Fire in the Cerrado 32,000 years ago. Current Research in the Pleistocene 11, 85–87.

Steig, E.J., 1999. Paleoclimate:Mid-Holocene climate change. Science 286, 1485–1487. doi:10.1126/science.286.5444.1485 URL http://www.sciencemag.org.

Thonicke, K., Prentice, I.C., Hewitt, C., 2005. Modelling glacial–interglacial changes in global fire regimes and trace gas emissions. Global Biogeochemical Cycles. doi:10.1029/2004GB0022782.

Viegas, D.X., Bovio, G., Ferreira, A., Nosenzo, A., Sol, B., 1999. Comparative study of various methods of fire danger evaluation in southern Europe. International Journal of Wildland Fire 9, 235–246.

Werth, J., Werth, P., 1998. Haines Index climatology for the western United States. Fire Management Notes 58, 8–17.

Whitlock, C., 2004. Forests, fires and climate. Nature 432, 28–29.

Whitlock, C., Bianchi, M.M., Bartlein, P.J., Markgraf, V., Marlon, J., Walsh, M., McCoy, N., 2006. Postglacial vegetation, climate, and fire history along the east side of the Andes (lat 41–42.5S), Argentina. Quaternary Research 66, 187–201.

Wilks, D.S., 1995. Statistical Methods in the Atmospheric Sciences: an Introduction. Academic Press, San Diego.

Wille, M., Negret, J.A., Hooghiemstra, H., 2000. Paleoenvironmental history of the Popayan area since 27,000 yr BP at Timbio, Southern Colombia. Review of Palaeobotany and Palynology 109, 45–63.

Winkler, J.A., Potter, B., Wilhelm, D., Shadbolt, R., Bian, X., Piromsopa, K., 2005. A climatology of the Haines Index for North America derived from NCEP/NCAR reanalysis fields. Sixth Fire and Forest Meteorology Symposium, American Meteorological Society.

Zhou, X., Mahalingam, S., 2001. Evaluation of a reduced mechanism for modeling combustion of pyrolysis gas in wildland fire. Combustion Science and Technology 171, 39–70.